International Journal of Nanomedicine

Dovepress
open access to scientific and medical research

Open Access Full Text Article

ORIGINAL RESEARCH

Ascorbyl palmitate/D-α-tocopheryl polyethylene glycol 1000 succinate monoester mixed micelles for prolonged circulation and targeted delivery of compound K for antilung cancer therapy in vitro and in vivo

This article was published in the following Dove Press journal:
International Journal of Nanomedicine
16 January 2017
Number of times this article has been viewed

Youwen Zhang
Deyin Tong
Daobiao Che
Bing Pei
Xiaodong Xia
Gaofeng Yuan
Xin Jin

Department of Hospital Pharmacy, The First Hospital of Suqian, Suqian, People's Republic of China

Abstract: The roles of ginsenoside compound K (CK) in inhibiting tumor have been widely recognized in recent years. However, low water solubility and significant P-gp efflux have restricted its application. In this study, CK ascorbyl palmitate (AP)/D-α-tocopheryl polyethylene glycol 1000 succinate monoester (TPGS) mixed micelles were prepared as a delivery system to increase the absorption and targeted antitumor effect of CK. Consequently, the solubility of CK increased from 35.2±4.3 to 1,463.2±153.3 μg/mL. Furthermore, in an in vitro A549 cell model, CK AP/TPGS mixed micelles significantly inhibited cell growth, induced G0/G1 phase cell cycle arrest, induced cell apoptosis, and inhibited cell migration compared to free CK, all indicating that the developed micellar delivery system could increase the antitumor effect of CK in vitro. Both in vitro cellular fluorescence uptake and in vivo near-infrared imaging studies indicated that AP/TPGS mixed micelles can promote cellular uptake and enhance tumor targeting. Moreover, studies in the A549 lung cancer xenograft mouse model showed that CK AP/TPGS mixed micelles are an efficient tumor-targeted drug delivery system with an effective antitumor effect. Western blot analysis further confirmed that the marked antitumor effect in vivo could likely be due to apoptosis promotion and P-gp efflux inhibition. Therefore, these findings suggest that the AP/TPGS mixed micellar delivery system could be an efficient delivery strategy for enhanced tumor targeting and antitumor effects.

Keywords: ginsenoside CK, ascorbyl palmitate, TPGS, mixed micelles, anti-tumor therapy

Introduction

Approximately 1.8 million new lung cancer cases and 1.6 million lung cancer-related deaths were reported in 2012, accounting for the highest reported incidence of mortality.[1] In an attempt to decrease the high mortality rate of lung cancer, more attention needs to be focused on finding alternative treatment methods.

Ginsenosides, the major active compounds of ginseng, have been widely used for different applications, especially for cancer.[2,3] Compound K (CK) is one of the major metabolites of ginsenosides that exhibits maximal antitumor effect.[4,5] However, its low water solubility, poor permeability, and significant P-gp efflux restrict its application.[6,7] Therefore, the goal of this study was to increase the solubility, targeted efficacy, and antitumor effect via formation of mixed micelles.

Correspondence: Xin Jin
Department of Hospital Pharmacy, The First Hospital of Suqian, 120 Suzhilu, Suqian 223800, People's Republic of China
Tel +86 159 5189 6676
Email jinxin871211@163.com

submit your manuscript | www.dovepress.com
Dovepress
http://dx.doi.org/10.2147/IJN.S119226

Binary mixed micelles of surfactants in aqueous solutions have wide applications. Lesser amounts of substance are used in the industrial application of such mixtures of surfactants than individual surfactants. The interactions between different units of mixed micelles could make it more stable.[8,9] In addition, the application of binary mixture of surfactants, especially for obtaining micellar solutions, by changing the molar fraction of the surfactants in their binary mixture, can lead to an increased solubility capacity of the micellar system.[10,11] D-α-Tocopheryl polyethylene glycol 1000 succinate monoester (TPGS) is a PEGylated vitamin E that has great advantages in enhancing the solubility and inhibiting P-gp efflux.[12,13] In addition, after micelle formation, it can escape recognition and elimination in vivo and has a prolonged circulation.[14] It is also generally regarded as a safe listed oral supplement, which has been approved by the US Food and Drug Administration as a safe pharmaceutical adjuvant used in drug formulation, and has been investigated for oral and parenteral administration in antineoplastic therapy.[14,15] Ascorbyl palmitate (AP), an amphiphilic derivative of ascorbic acid that has antioxidant activity, can also self-aggregate and form micellar structures in aqueous media.[16,17] Ascorbate has been shown to increase the effectiveness of various anticancer treatments.[18,19] Mixed micelles composed of TPGS and AP are nanosized colloidal particles with a hydrophobic core and a hydrophilic corona. The hydrophobic segment forms the core of the micelles that solubilize the hydrophobic drug molecules, and the hydrophilic segment forms the corona that provides compatibility of the micelles in the aqueous environment. The hydrophobic core accommodates various hydrophobic molecules, such as therapeutics and imaging agents, thus improving the solubility and stability in the biological system.[20,21] The hydrophilic corona shields the core and protects the loaded drugs from interactions with the blood components. The biocompatible polymeric corona causes reduced recognition of the micelles by reticuloendothelial systems, thus providing prolonged circulation of the loaded component in the blood stream.[22,23] The nanoranged size along with the prolonged circulatory property allows mixed micelles to eventually accumulate in any compromised tissue vasculature sites, eg, tumor via a passive targeting phenomenon commonly referred to as enhanced permeability and retention effect.[20,22,24]

Therefore, the overarching aim of the current study was to design a novel AP/TPGS mixed micellar system and investigate its potential targeted therapeutic effect in treating lung cancer in vitro and in vivo. The AP/TPGS mixed micelles of CK could enhance the water solubility and permeability of CK, prolong its retention time, and promote its accumulation in tumor tissues. It could be a potential alternative for effective and targeted tumor therapy.

Materials and methods

Preparation and characterization of CK mixed micelles

CK-loaded AP/TPGS mixed micelles were prepared as follows: CK, TPGS, and AP were dissolved in ethanol to form a clear solution. Then, the organic solvent was evaporated under vacuum at 40°C to form a thin film. The thin film was hydrated by deionized water for 30 min at 40°C to form the mixed micelles. 1,1′-dioctadecyl-3,3,3′, 3′-tetramethylindotricarbocyanine iodide (DiR) mixed micelles and coumarin-6 mixed micelles were also prepared by the abovementioned method with the substitution of DiR and coumarin-6 for CK, respectively.

Particle size, polydispersity, and morphology

Size, zeta potential, and polydispersity of the CK mixed micelles were determined using Malvern Zetasizer Instruments (Nano ZS; Malvern Instruments, Malvern, UK). A total of 2 mL of mixed micelles was taken in a polystyrene disposable cuvette and exposed to laser light diffraction at an angle of 90° to determine size and polydispersity. A total of 1 mL of mixed micelles was placed in the electrophoretic cell of the Malvern Zetasizer Nano ZS and the average surface charge was determined. To verify the reproducibility of results, the experiments were performed in triplicate.

Morphology of the mixed micellar formulations was observed using a transmission election microscope (JEM 100CX, JEOL, Tokyo, Japan).

The drug loading content (LC) of mixed micelles

The drug LC was measured by a high-performance liquid chromatography (HPLC) method. The mixed micelles were spun down at 13,000× *g* for 15 min; 200 µL of the supernatants was diluted in 800 µL of methanol and analyzed for CK.

The drug LC and encapsulation efficiency (EE) of CK mixed micelles were calculated using the following formulae:

$$\text{LC}\ (\%) = \frac{\text{Mass of CK encapsulated in micelles}}{\text{Mass of mixed micelles}} \times 100\%$$

$$\text{EE}\ (\%) = \frac{\text{Mass of CK in micelles}}{\text{Mass of feeding CK}} \times 100\%.$$

Solubility measurements

Classical approaches for measuring solubility are based on the saturation shake-flask method. Excess amounts of CK were placed into 5 mL vials containing aqueous solutions. The vials were sealed and placed into a constant temperature bath (37°C) and shaken for 24 h, until equilibrium was evident. After centrifugation of the incubated suspensions at 37°C and 15,000 rpm for 15 min, the concentrations of CK in the supernatant solutions were determined by an HPLC procedure, and the concentration of CK in the micellar system was determined after a 100 times dilution with methanol and then analyzed for CK.

Stability of CK mixed micelles

A total of 100 μL of CK mixed micelles was diluted with phosphate buffered saline (PBS) buffer (pH 7.4) to 1 mL and incubated at 37°C for 7 days. The variance of particle size and solubility were measured once a day.

In vitro drug release

The in vitro drug release of the CK mixed micelles was evaluated by dialysis bag diffusion. The CK mixed micelles at a volume equivalent to 50 mg of free CK were added to a dialysis bag and immersed into 50 mL of PBS containing 0.2% w/v Tween 80 with continuous shaking at 100 rpm at 37°C. Isopycnic fresh medium was replaced after withdrawal from the receptor compartment. The samples were filtered through a 0.45 μm syringe filter before being transferred into an HPLC vial.

In vitro cellular uptake

Following incubation of A549 cells (purchased from Nanjing KeyGen Biotech Co. Ltd, Nanjing, People's Republic of China) in glass-bottomed dishes containing culture medium at 37°C for 24 h, cell culture media containing coumarin-6 solution and coumarin-6-loaded mixed micelles were added and incubated for 4 h at 37°C. The A549 cells were washed with ice-cold PBS twice and fixed with 95% ethanol for 20 min. Then, the cells were fixed with paraformaldehyde and stained with 4′,6-diamidino-2-phenylindole (DAPI) for 15 min. The fluorescent images of the cells were observed under a fluorescence microscope (IX71; Olympus Corp, Tokyo, Japan) and a Leica confocal laser scanning microscope (CLSM; TCS SP5; Leica, Heidelberg, Germany).

Cell viability assay

Cells were seeded in 96-well plates and treated with CK or CK mixed micelles. The different concentrations of CK or CK mixed micelles were 5, 10, 20, 40, and 80 μg/mL. The untreated cells were used as control for this study. After incubation for 24 h, the cells were stained with 3-(4,5-dimethyl-2-thiazolyl)-2,5-diphenyl-2-H-tetrazolium bromide for 4 h. The blue crystals in cells were dissolved with dimethyl sulphoxide. The absorbance intensity was then measured using a microplate reader at an absorbance wavelength of 570 nm after subtracting the background absorbance at 660 nm.

TUNEL analysis

DNA fragmentation was detected in situ by TUNEL staining. Briefly, after being treated with CK or CK mixed micelles, A549 cells were permeabilized by Tris-HCl and ethylenediaminetetraacetic acid (EDTA) for 10 min. The cells were then washed, fixed, and labeled with TUNEL reaction mixture at 37°C for 60 min in the dark. The nuclei of apoptotic cells were stained brown. However, the nuclei of normal cells were purple. The morphology of cells was recorded by photography.

Cell apoptosis

A549 cells were incubated with CK or CK mixed micelles at a CK concentration of 10 μg/mL for 24 h. After washing twice with ice-cold PBS, the cells were harvested with trypsin–EDTA and resuspended at 1×10^6 cells/mL. Cell suspensions (100 μL) were kept in the dark and stained simultaneously with fluorescein isothiocyanate-annexin V and propidium iodide (PI) for 10 min at 37°C, and then apoptosis was analyzed by flow cytometry.

Cell cycle analysis

A549 cells were seeded into 6-well plates and cultured. After exposure to CK or CK mixed micelles at 10 μg/mL of CK for 24 h, A549 cells were harvested with trypsin–EDTA. After washing twice with ice-cold PBS, the cells were fixed with 70% ethanol and stored at 4°C for 12 h. Before analyzing the DNA content, samples were suspended in 1.0 mL hypotonic PI solution, and incubated in the dark for 30 min prior to flow cytometric analysis.

Cell migration assay

A549 cells were seeded onto a 12-well plate to obtain a cell monolayer. A 200 μL pipette tip was then used to produce a vertical wound. Wounded cells were removed by gently washing twice with PBS. Then, free CK or CK mixed micelles in serum-free medium was added to the cells, which were incubated for an additional 24 h. The cells were photographed, and the width of the wound was evaluated using a microscope.

Animals

Nude mice (20±2 g body weight) were purchased from SLEK Lab Animal Center of Shanghai (Shanghai, People's Republic of China). All animal experiments were performed in accordance with institutional principles of care and use of laboratory animals (revised according to the national standard) and were approved by the experimental animal administrative committee of The First Hospital of Suqian. We confirm that ethical and legal approval was obtained prior to the commencement of the study.

Targeted effect of DiR-loaded mixed micelles in vivo

A549 cell suspension was inoculated into nude mice via a hypodermic injection, and the mice were divided into two groups (n=3) when the tumor volume reached ~150 mm^3. The mice were then administered DiR or DiR mixed micelles via tail vein injections for imaging study, anesthetized via isoflurane, and evaluated at 1, 2, 4, 8, 12, and 24 h using the IVIS 200 imaging system (PerkinElmer, Hopkinton, MA, USA) at an excitation/emission wavelength of 625/700 nm, respectively. The exposure time was 30 s per image. After in vivo imaging, the major tissues were obtained to determine the associated fluorescence intensities for ex vivo imaging.

Antitumor efficacy in lung cancer xenografts

Nude mice were used for investigating the antitumor efficacy in vivo when tumor volume reached 50 mm^3. The mice were randomly divided into three treatment groups (five in each group). Then, saline, CK (30 mg/kg), or CK mixed micelles (30 mg/kg) were administered via tail vein injections every 3 days until the 12th day. The tumor volumes and body weight were recorded every 3 days until the 15th day. Tumor volumes were calculated as length × $width^2/2$ (mm^3). At the end of the experiment, the tumor, liver, and kidney were obtained for pathological study by hematoxylin and eosin (H&E).

Western blot analysis

The tumor cell lysates were separated by sodium dodecyl sulfate polyacrylamide gel electrophoresis (SDS-PAGE) and transferred onto polyvinylidene difluoride (PVDF) membranes. The membranes were incubated with specific primary antibodies at 4°C for 12 h and visualized using a Western blotting detection system. Caspase 3, caspase 8, caspase 9, P-gp, Bax, and Bcl-2 antibodies were obtained from Santa Cruz Biotechnology, Inc. (Santa Cruz, CA, USA). The results of Western blot were analyzed by gray level of chemiluminescence.

Statistical analysis

Data are presented as mean ± standard deviation (SD). Student's *t*-tests for two-group comparisons were performed to determine the statistical significance ($P<0.05$).

Results and discussion

Characterization of CK mixed micelles

The sizes and morphology of CK mixed micelles are illustrated in Figure 1. The average size of CK mixed micelles was 30.28±4.15 nm with a low polydispersity (Figure 1A). The CK mixed micelles had the highest negative zeta potential (–27.1±2.84 mV). The morphological images showed that CK mixed micelles were nanometer sized and spherical (Figure 1B). The drug LC was 13.26%±1.89% with a high entrapment efficiency (91.34%±5.24%). The solubility of CK increased from 35.2±4.3 to 1,463.2±153.3 μg/mL after CK AP/TPGS mixed micelle formation. Both the sizes of CK mixed micelles and the solubility of CK exhibited no significant decrease in 7 days. This shelf life could result in much convenience for the CK mixed micelles' application. Furthermore, in vitro, a significantly higher release was reported for free CK group than that for CK mixed micelles, as shown in Figure 1C. This may be due to surface PEGylation and controlled release of mixed micelles group.

In vitro cellular uptake

Both fluorescence microscopy and confocal microscopy were used to confirm the uptake of mixed micelles in tumor cells by taking advantage of the intrinsic fluorescence of coumarin-6 and DAPI as the fluorescent probes. Figures 2 and 3 show that the nuclei of A549 cancer cells were stained blue with DAPI, while the cytoplasm was stained green with coumarin-6. After incubation with coumarin-6 for 4 h, the fluorescence images of A549 cell lines were photographed. In the free CK coumarin-6 group, the cytoplasm showed decreased green fluorescence. However, for the coumarin-6 mixed micelles group, the images showed a more intense fluorescence in cytoplasm. The observation indicated that mixed micelles could promote drug uptake. However, there was no significant accumulation of coumarin-6 in the cell nuclei.

In vitro cytotoxicity

The results for in vitro cytotoxicity are shown in Figure 4A; both free CK and CK mixed micelles have dose-dependent inhibitory effects on the viability of A549 cells. CK mixed micelles showed noticeable cytotoxicities in A549 tumor cells after 24 h incubation. The inhibition efficacy of CK mixed micelles against cell proliferation is better than that of free CK. The half-maximal inhibitory concentration (IC_{50})

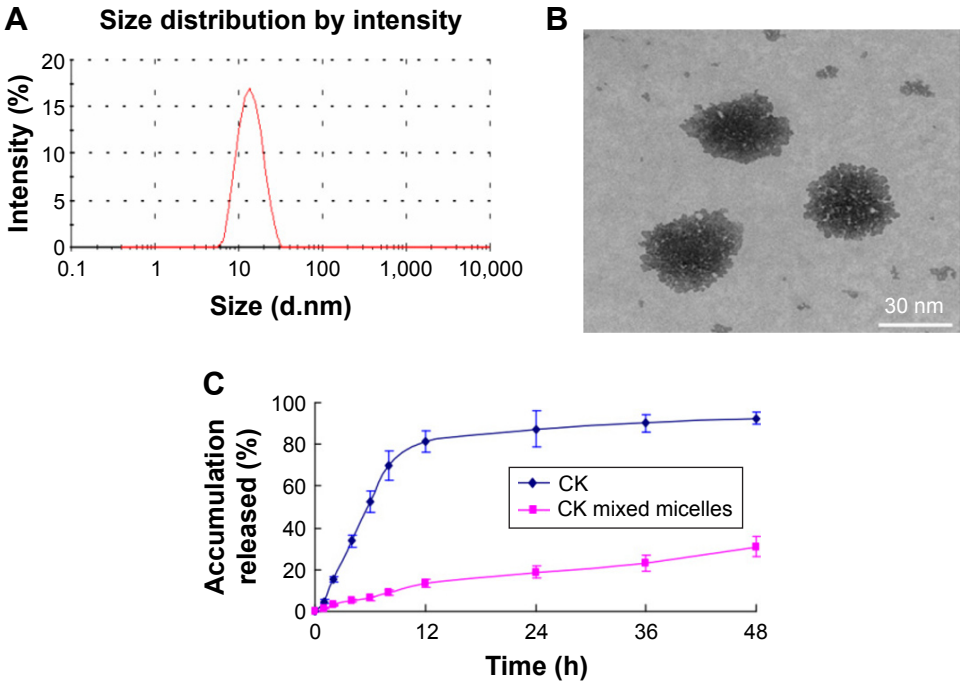

Figure 1 Droplet size (**A**), morphology (**B**) of CK mixed micelles, and its release in vitro (**C**).
Note: n=3, mean ± SE.
Abbreviations: CK, compound K; SE, standard error; h, hours.

of free CK and CK mixed micelles at 24 h was 16.11±1.23 and 10.29±1.17 μg/mL, respectively. The results showed that formation of CK mixed micelles could increase the antitumor activity of CK. However, a similar tendency was not observed for CK release, which suggests that the improved antitumor effect of CK mixed micelles could likely be attributable to improved drug delivery instead of drug release.

TUNEL assay

The TUNEL assay was used to evaluate the DNA damage in situ. Its indication of apoptosis could specifically infer DNA strand breaks in cells. As shown in Figure 4B, both free CK and CK mixed micelles significantly induced cell apoptosis as revealed by cells with brown-stained nuclei as compared with control ($P<0.05$), while the normal cells were stained blue and had a low apoptosis index. In the CK micelle group, the apoptosis index was 45%±5.25%, which is significantly larger than that in the CK group (17.28%±2.25%), also indicating that mixed micelle nanocarriers exhibited better apoptosis effect to promote the antitumor effect.

Apoptosis in A549 cells

Next, to further analyze apoptosis, flow cytometry was chosen to quantify the proportion of cells in early and

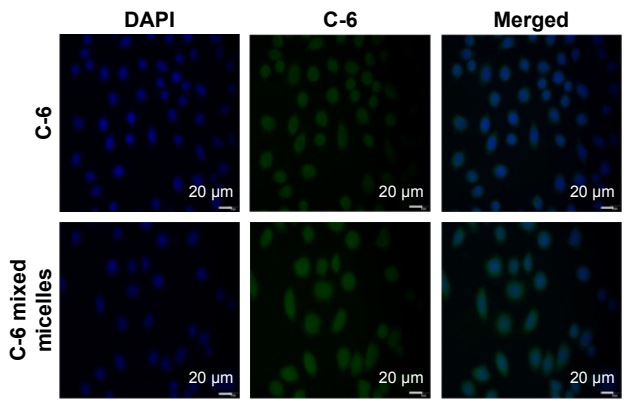

Figure 2 Fluorescence microscopy of A549 cell following 4 h of treatment with C-6 or C-6 mixed micelles (n=3).
Abbreviations: C-6, coumarin-6; DAPI, 4′,6-diamidino-2-phenylindole; h, hours.

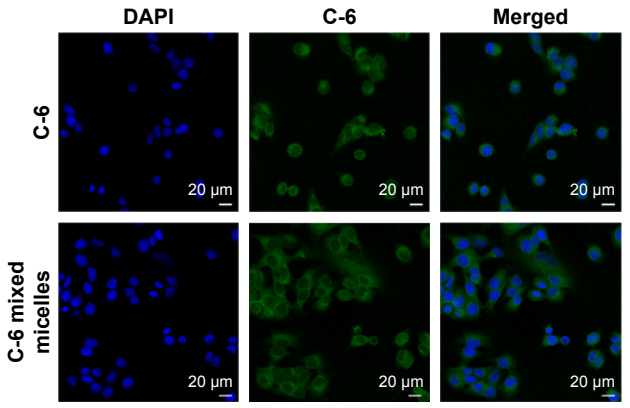

Figure 3 Confocal microscopy of A549 cell following 4 h of treatment with C-6 or C-6 mixed micelles (n=3).
Abbreviations: C-6, coumarin-6; DAPI, 4′,6-diamidino-2-phenylindole; h, hours.

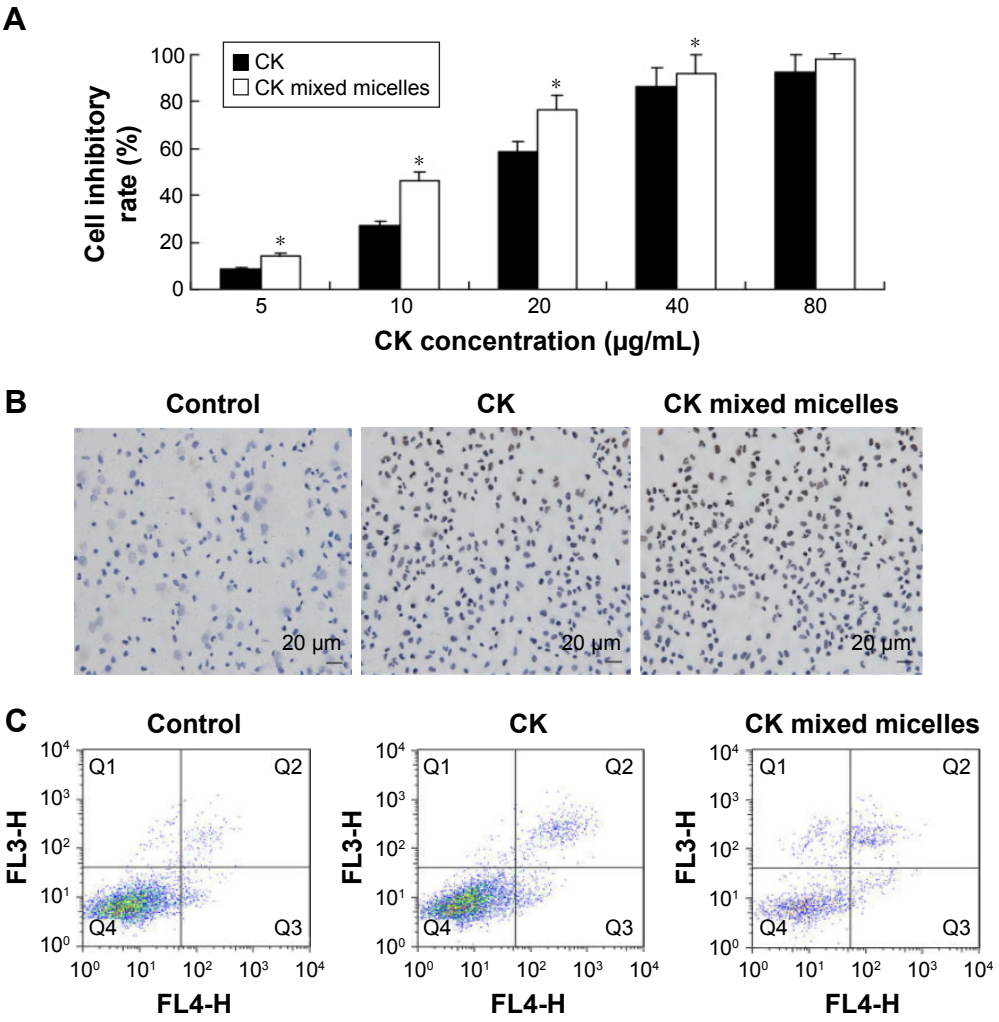

Figure 4 (**A**) Antitumor effect of CK and CK mixed micelles to A549 cell on different concentrations. *$P<0.05$ CK versus CK mixed micelle at same concentration. The apoptosis of A549 cell was determined by TUNEL (**B**) and annexin V-FITC/PI staining (**C**) (n=3, mean ± SE).
Abbreviations: CK, compound K; SE, standard error; PI, propidium iodide; FITC, fluorescein isothiocyanate.

late-stage apoptosis. As shown in Figure 4C, in the control group, the proportion of late-stage apoptotic A549 cells was 2.63%±0.28%. No significant apoptosis was observed in the control group. On the contrary, the proportion of late-stage apoptotic cells for free CK and CK mixed micelles was 7.34%±1.51% and 16.59%±2.83%, respectively, which indicates a significant increase. The tendency of early apoptosis was similar to late apoptosis mentioned earlier. Thus, CK mixed micelles were found to induce cell apoptosis markedly both in early and late stages of apoptosis compared with CK group.

Cell cycle distribution in A549 cells

The other possible effect of CK and CK mixed micelles was investigated. The percentage of cells in phase of cell cycle was significantly altered by CK or CK mixed micelles (Figure 5A). The micelles induced G0/G1 arrest in rapidly dividing cells, eventually resulting in better effect than CK.

Cell migration assay

Wound-healing assay was used to evaluate the effect on cell migration. The untreated group had a small wound after 24 h, but for the CK or CK mixed micelles group, a large wound was observed, indicating significant migration inhibition (Figure 5B). Thus, the CK mixed micelles exhibited better antimigration effect than CK.

Near-infrared fluorescence imaging

As seen in Figure 6, in vivo fluorescent optical imaging revealed weak fluorescence intensity in the tumor tissue for the DiR group, while in the DiR mixed micelles group, the fluorescence intensity significantly increased. DiR mixed

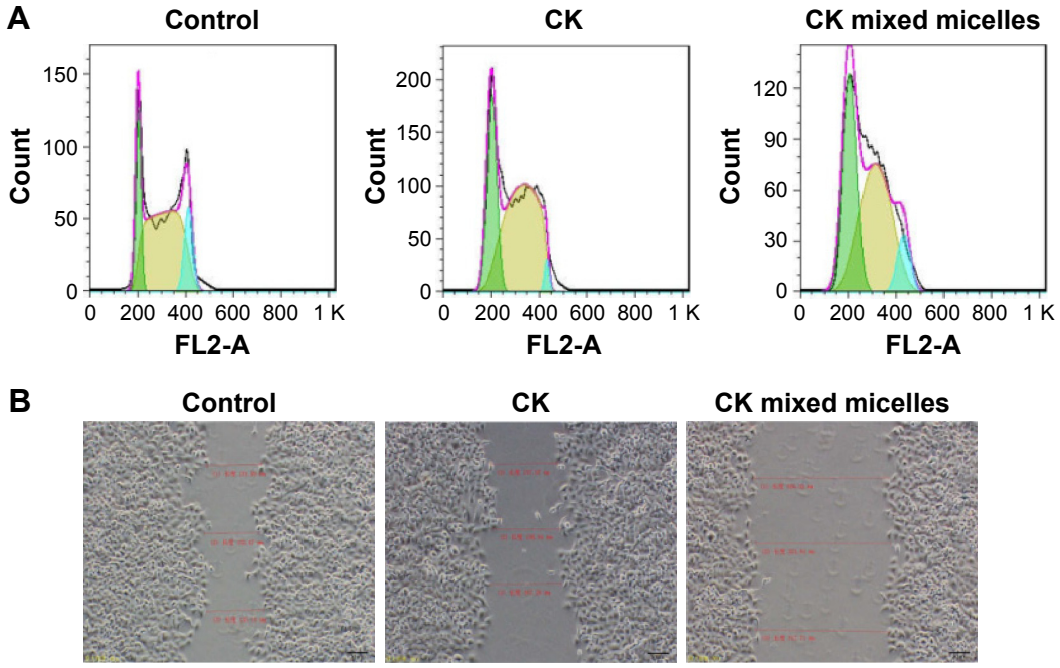

Figure 5 Cell cycle analysis assay (green G1, brown S, and blue G2 phase). (**A**) and wound healing assay (**B**) on A549 cell.
Notes: n=3, mean ± SE. Scale 50 μm.
Abbreviations: CK, compound K; SE, standard error.

micelles displayed better targeting efficiency compared to free DiR, as evidenced by the fluorescence at 2 h after injection and maximum absorbance at 8 h. Furthermore, DiR mixed micelles exhibited low clearance until 24 h with strong fluorescence in tumor tissue. It can be inferred that DiR mixed micelles possessed better tumor targeting with a prolonged circulation effect. To further confirm the tissue distribution, ex vivo imaging of major tissues was performed and showed that the uptake of DiR by the tumor cells increased up to 24 h from the mixed micelles due to the targeting effect.

Assessment of in vivo therapeutic efficacy

At the end of the experiment, the tumor volumes of the CK or CK mixed micelles group were all notably lower than those of the control group (Figure 7A and B). A significant difference in tumor volumes was observed among all groups. The CK mixed micelles exhibited the maximal antitumor effect (66.24%±8.77% at day 15). In order to evaluate the adverse effects of CK or CK mixed micelles, body weight was also recorded during the experiment. No significant changes in average body weight were observed until day 15.

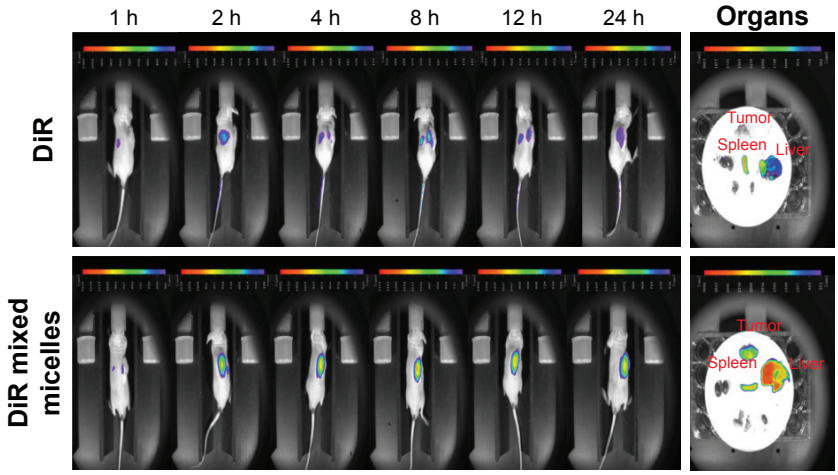

Figure 6 In vivo imaging studies for tumor targeting ability of DiR mixed micelles (n=3).
Abbreviations: DiR, 1,1′-dioctadecyl-3,3,3′,3′-tetramethylindotricarbocyanine iodide; h, hours.

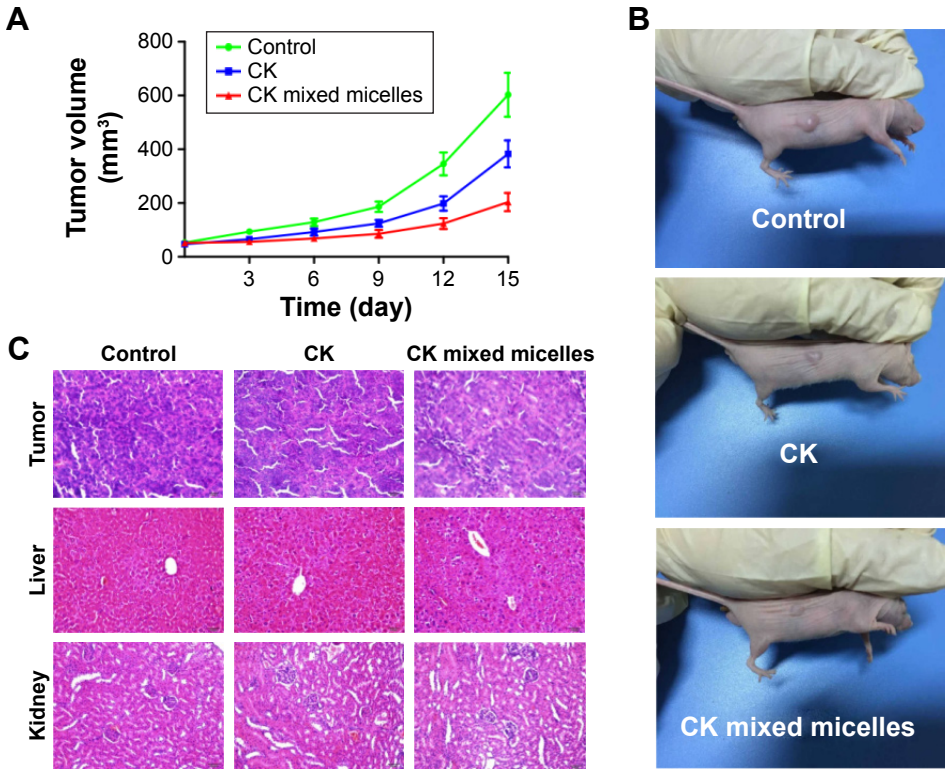

Figure 7 The relative tumor volume–time curve (**A**). Photographs of tumors from different formations at the end of the experiment (**B**). Hematoxylin and eosin assay of the excised tumor, liver and kidney from subcutaneous tumor-bearing nude mice at the end of the experiment (**C**) (n=5, mean ± SE).
Abbreviations: CK, compound K; SE, standard error.

The improved antitumor efficacy of CK mixed micelles in mice was further confirmed by histopathology analysis. H&E assay was chosen to further evaluate antitumor efficacy, hepatic toxicity, and renal toxicity (Figure 7C). CK mixed micelles exhibited the most effective antitumor activity. Morphological analysis of tumor slices of the CK mixed micelles group showed significant nuclear pyknosis and karyorrhexis, which indicate prominent apoptosis promoting effect consistent with the in vitro study. The pathological analysis of the liver and kidney showed no significant difference compared with the results observed for the control group. The abovementioned results show that the CK mixed micelles had better antitumor efficacy with lower hepato and renal toxicity.

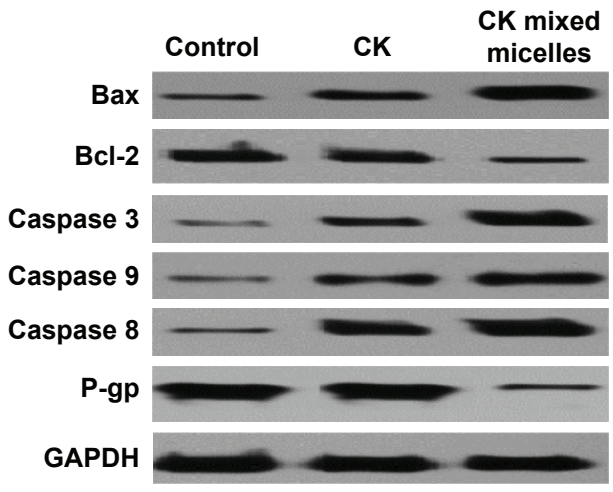

Figure 8 Expression of proteins associated with apoptosis and efflux were analyzed by Western blotting (n=5).
Abbreviation: CK, compound K.

As shown in Figure 8, treatment with CK mixed micelles significantly increased BAX expression and decreased Bcl-2 expression. Compared with the free CK group, the CK mixed micelles group showed almost 7.25-fold increase in BAX/Bcl-2 ratio. This indicated that CK mixed micelles could promote cell apoptosis via increased accumulation in tumor. The expression of caspase 3, caspase 8, and caspase 9 in tumor cells was detected to evaluate the upregulation of apoptosis sensitivity. The most favorable effect was observed in the CK mixed micelles group. The gray value of caspase 3, caspase 8, and caspase 9 increased by almost 100% in the CK mixed micelles group, compared to that in the free CK group. Interestingly, P-gp expression in tumors significantly decreased in the CK mixed micelles group, likely owing to the P-gp efflux inhibitory activity of TPGS.

At tumor sites, the overproduction of oxyradical has been reported. Mixed micelles contained antioxidants that may promote nanocarrier uptake by neutralizing the peroxides in tumor internal environment.[25] This interaction could decrease oxidative stress and promote treatment efficacy at tumor sites.[26–28] Moreover, unlike most normal vasculature, tumor vasculature has prevalent leaky vascular endothelium because of uncontrolled growth. Nanoparticles can effectively pass through the tumor vasculature because of the enhanced permeability and retention effect.[29] In addition, particles with a diameter range of ~10–30 nm can avoid the accelerated blood clearance phenomenon and accordingly realize the prolonged circulation effect.[30,31] Furthermore, PEGylation on the surface of mixed micelles can increase the uptake and circulation in vivo.[32] Therefore, according to the abovementioned effects, the AP/TPGS mixed micelles were easily extravasated at tumor sites for passive targeted effect with prolonged circulation to increase antitumor effect in vivo. However, the use of AP as an antioxidant for facilitating targeted tumor tissue needs further research.

Conclusion

We aimed to evaluate the anticancer function and mainly focus on the promotion of apoptosis, cellular uptake, and tumor targeted effect of CK AP/TPGS mixed micelles. The in vitro and in vivo studies both indicated that the antitumor effect of the CK increased following the formation of the AP/TPGS mixed micelles. Therefore, AP/TPGS mixed micelles of CK could be a potential alternative for effective and targeted tumor therapy.

Acknowledgment

This work was supported by National Natural Science Foundation of China (Grant No 81403119), 333 project of Jiangsu Province and the Science and Technology Support Project of Suqian (S210520).

Disclosure

The authors report no conflicts of interest in this work.

References

1. Torre LA, Bray F, Siegel RL, Ferlay J, Lortet-Tieulent J, Jemal A. Global cancer statistics, 2012. *CA Cancer J Clin*. 2015;65(2):87–108.
2. Ru W, Wang D, Xu Y, et al. Chemical constituents and bioactivities of panax ginseng (C. A. Mey.). *Drug Discov Ther*. 2015;9(1):23–32.
3. Wong AS, Che CM, Leung KW. Recent advances in ginseng as cancer therapeutics: a functional and mechanistic overview. *Nat Prod Rep*. 2015; 32(2):256–272.
4. Wang CZ, Cai Y, Anderson S, Yuan CS. Ginseng metabolites on cancer chemoprevention: an angiogenesis link? *Diseases*. 2015;3(3): 193–204.
5. Yang XD, Yang YY, Ouyang DS, Yang GP. A review of biotransformation and pharmacology of ginsenoside compound K. *Fitoterapia*. 2015;100:208–220.
6. Zhang B, Zhu XM, Hu JN, et al. Absorption mechanism of ginsenoside compound K and its butyl and octyl ester prodrugs in Caco-2 cells. *J Agric Food Chem*. 2012;60(41):10278–10284.
7. Yang Z, Wang JR, Niu T, et al. Inhibition of P-glycoprotein leads to improved oral bioavailability of compound K, an anticancer metabolite of red ginseng extract produced by gut microflora. *Drug Metab Dispos*. 2012;40(8):1538–1544.
8. Poša M, Popović K, Ćirin D, Agatić ZF. Binary mixed micelles of triton X-100 and selected bile salts: thermodynamic stabilization and pKa values of micellar bile acids. *J Chem Thermodyn*. 2016;103:333–341.
9. Lukowicz T, Maldonado RC, Molinier V, Aubry JM, Nardello-Rataj V. Fragrance solubilization in the temperature insensitive aqueous microemulsions based on synergistic mixtures of nonionic and anionic surfactants. *Colloids Surf A Physiochem Eng Aspects*. 2014;458:85–95.
10. Ebrahim Attia AB, Ong ZY, Hedrickc JL, et al. Mixed micelles self-assembled from block copolymers for drug delivery. *Curr Opin Colloid Interface Sci*. 2011;16:182–194.
11. Poša M, Popović K, Ćirin D, Farkaš Z. Binary mixed micelles of polysorbates (Tween 20 and Tween 60) and bile salts (Na-hyodeoxycholate and Na-cholate): regular solution theory and change of pKa values of micellar bile acid – a novel approach to estimate of the stability of the mixed micelles. *Fluid Phase Equilibr*. 2015;396:1–8.
12. Duhem N, Danhier F, Préat V. Vitamin E-based nanomedicines for anti-cancer drug delivery. *J Control Release*. 2014;182:33–44.
13. Butt AM, Mohd Amin MC, Katas H. Synergistic effect of pH-responsive folate-functionalized poloxamer 407-TPGS-mixed micelles on targeted delivery of anticancer drugs. *Int J Nanomedicine*. 2015;10: 1321–1334.
14. Shen R, Kim JJ, Yao M, Elbayoumi TA. Development and evaluation of vitamin E D-α-tocopheryl polyethylene glycol 1000 succinate-mixed polymeric phospholipid micelles of berberine as an anticancer nanopharmaceutical. *Int J Nanomedicine*. 2016;11:1687–1700.
15. Fiorella T, Cristal CC, Jimena S, et al. Characterization and biodistribution of bevacizumab TPGS-based nanomicelles: preliminary studies. *J Drug Deliv Sci Tec*. 2016;36:95–98.
16. Venkat Ratnam D, Ankola DD, Bhardwaj V, Sahana DK, Ravi Kumar MNV. Role of antioxidants in prophylaxis and therapy: a pharmaceutical perspective. *J Control Release*. 2006;113(3):189–207.
17. Sánchez Vallecillo MF, Minguito de la Escalera MM, Aguirre MV, et al. A liquid crystal of ascorbyl palmitate, used as vaccine platform, provides sustained release of antigen and has intrinsic pro-inflammatory and adjuvant activities which are dependent on MyD88 adaptor protein. *J Control Release*. 2015;214:12–22.
18. Chen Q, Polireddy K, Chen P, Dong R. The unpaved journey of vitamin C in cancer treatment. *Can J Physiol Pharmacol*. 2015;93(12): 1055–1063.
19. Venturelli S, Sinnberg TW, Niessner H, Busch C. Molecular mechanisms of pharmacological doses of ascorbate on cancer cells. *Wien Med Wochenschr*. 2015;165(11–12):251–257.
20. Biswas S, Kumari P, Lakhani PM, Ghosh B. Recent advances in polymeric micelles for anti-cancer drug delivery. *Eur J Pharm Sci*. 2016;83: 184–202.
21. Gothwal A, Khan I, Gupta U. Polymeric micelles: recent advancements in the delivery of anticancer drugs. *Pharm Res*. 2016;33(1):18–39.
22. Reddy BP, Yadav HK, Nagesha DK, Raizaday A, Karim A. Polymeric micelles as novel carriers for poorly soluble drugs – a review. *J Nanosci Nanotechnol*. 2015;15(6):4009–4018.
23. Movassaghian S, Merkel OM, Torchilin VP. Applications of polymer micelles for imaging and drug delivery. *Wiley Interdiscip Rev Nanomed Nanobiotechnol*. 2015;7(5):691–707.
24. Sosnik A, Menaker Raskin M. Polymeric micelles in mucosal drug delivery: challenges towards clinical translation. *Biotechnol Adv*. 2015; 33(6 pt 3):1380–1392.

25. Yin TJ, Wang L, Yin LF, Zhou JP, Huo MR. Co-delivery of hydrophobic paclitaxel and hydrophilic AURKA specific siRNA by redox-sensitive micelles for effective treatment of breast cancer. *Biomaterials*. 2015;61:10–25.
26. D'Souza GG, Wang T, Rockwell K, Torchilin VP. Surface modification of pharmaceutical nanocarriers with ascorbate residues improves their tumor-cell association and killing and the cytotoxic action of encapsulated paclitaxel in vitro. *Pharm Res*. 2008;25(11):2567–2572.
27. Hashizume H, Baluk P, Morikawa S, et al. Openings between defective endothelial cells explain tumor vessel leakiness. *Am J Pathol*. 2000;156(4):1363–1380.
28. Gopinath D, Ravi D, Rao BR, Apte SS, Renuka D, Rambhau D. Ascorbyl palmitate vesicles (aspasomes): formation, characterization and applications. *Int J Pharm*. 2004;271(1–2):95–113.
29. Fang J, Nakamura H, Maeda H. The EPR effect: unique features of tumor blood vessels for drug delivery, factors involved, and limitations and augmentation of the effect. *Adv Drug Deliv Rev*. 2011;63(3):136.e51.
30. Koide H, Asai T, Hatanaka K, et al. Particle size-dependent triggering of accelerated blood clearance phenomenon. *Int J Pharm*. 2008;362:197.e200.
31. Koide H, Asai T, Kato H, et al. Size-dependent induction of accelerated blood clearance phenomenon by repeated injections of polymeric micelles. *Int J Pharm*. 2012;432:75.e9.
32. Gao Z, Zhang L, Sun Y. Nanotechnology applied to overcome tumor drug resistance. *J Control Release*. 2012;162:45.e55.